Applied Catalysis B: Environmental 86 (2009) 87–92

Contents lists available at ScienceDirect

Applied Catalysis B: Environmental

journal homepage: www.elsevier.com/locate/apcatb

Characteristics of $Pt/WO_3/CeO_2/ZrO_2$ catalysts for catalytic reduction of NO by CO

Hai-ou Zhu, Jeong-Rang Kim, Son-Ki Ihm *

Department of Chemical and Biomolecular Engineering, Korea Advanced Institute of Science and Technology, 373-1, Guseong-dong, Yuseong-gu, Daejeon 305-701, Republic of Korea

ARTICLE INFO

Article history:
Received 14 December 2007
Received in revised form 8 July 2008
Accepted 25 July 2008
Available online 5 August 2008

Keywords:
Pt
CeO_2
ZrO_2
CeO_2–ZrO_2
Precipitation
WO_3
NO + CO reaction
Excess oxygen
Acidity
Pt dispersion

ABSTRACT

Various supported Pt catalysts ($Pt/WO_3/CeO_2/ZrO_2$; Pt/ZrO_2, Pt/CeO_2, Pt/CeZrO, $Pt/WO_3/ZrO_2$, and Pt/WO_3/CeZrO) were prepared and characterized, and their characteristics of catalytic reductions of NO by CO with or without oxygen were investigated. TPR and CO-TPD showed that Pt/CeO_2 and Pt/CeZrO could be easily reduced by CO while the reduction by CO was inhibited with the introduction of WO_3 in the case of Pt/WO_3/CeZrO. According to NO-TPD, NO reduction could not proceed over the catalysts (Pt/WO_3/CeZrO, Pt/ZrO_2, $Pt/WO_3/ZrO_2$) to remain in an oxidized state even after reduction by CO, but NO reduction was possible over Pt/CeO_2 and Pt/CeZrO catalysts when reduced by CO. For NO + CO reaction without oxygen, those easily reducible catalysts (Pt/CeO_2 and Pt/CeZrO) exhibited better catalytic performances. With excess oxygen, however, Pt/WO_3/CeZrO and $Pt/WO_3/ZrO_2$ catalysts exhibited higher NO conversions to N_2 and N_2O especially at a low temperature. The acidity from ZrO_2 and WO_3 in $Pt/WO_3/CeO_2/ZrO_2$ catalysts should play an important role on their NO conversion only in the presence of excess oxygen.

1. Introduction

Nowadays the catalytic reduction of NO by CO has attracted much attention for reducing NO_x emissions from automotive gas, and many researches using noble metal catalysts (Rh, Pt and Pd) were reported recently [1–7]. Due to the scarcity and high price of Rh, Pt was considered to be a better catalytic candidate for the catalytic reduction of NO.

Since CeO_2 had a good thermal stability and could enhance the migration and exchange of oxygen species by storing and releasing oxygen, it should be a proper support for Pt catalyst [8]. In order to improve the limitation that CeO_2 was sintered at 750 °C [9], some Ce atoms in its crystal lattice were replaced by other cations (such as Zr). This replacement would lead to the microstrain which should improve thermal stability as well as oxygen exchanging ability [10–14]. A new generation of mixed oxides based on CeO_2 and ZrO_2 has been developed recently. Since these kinds of catalysts could exchange the oxygen with reactants and were somewhat important for the redox reactions, the oxygen storage capacity (OSC) would be an important factor in exploring their catalytic performance. However, Pt catalyst supported on CeO_2–ZrO_2 mixed oxide has not been widely investigated in the catalytic reduction of NO by CO so far.

As reported by Regalbuto and Wolf [15], the addition of WO_3 to Pt/SiO_2 was believed to produce a small number of Pt-WO_3 adlineation sites having very high NO dissociation activity and increased the activity toward the NO–CO reaction. Perez-Hernandez et al. [16] suggested that the acid–basic sites on Pt/ZrO_2-CeO_2 catalysts were important for NO + CO reaction; while the acid properties, generated by zirconia content in the support, seemed to be important for NO + CH_4 reaction. Also several studies have demonstrated the importance of the acidic sites in the NO + CH_4 reaction [17–19]. Other authors have reported that the role of acid sites is to promote the NO oxidation step [20–24] on NO reduction with hydrocarbon. However, WO_3 supported on ZrO_2 can produce super-acidic sites and the effect of acidity from ZrO_2 and WO_3 is worth to be investigated.

In this work, the $Pt/WO_3/CeO_2/ZrO_2$ catalysts (Pt/ZrO_2, Pt/CeO_2, Pt/CeZrO, $Pt/WO_3/ZrO_2$, and Pt/WO_3/CeZrO) were prepared and their catalytic activities for NO + CO reaction with or without oxygen were discussed in terms of redox property and acidity measured by temperature-programmed experiments.

* Corresponding author. Tel.: +82 42 869 3915; fax: +82 42 869 5955.
E-mail address: skihm@kaist.ac.kr (S.-K. Ihm).

0926-3373/$ – see front matter © 2008 Elsevier B.V. All rights reserved.
doi:10.1016/j.apcatb.2008.07.024

2. Experimental

2.1. Preparation of catalysts

CeO_2, ZrO_2, and CeZrO (CeO_2–ZrO_2 mixed oxides, mole ratio of Ce:Zr = 0.65:0.35) were prepared by a precipitation method. $ZrO(NO_3)_2$ and $Ce(NO_3)_3$ (Aldrich Chemical Company) were used as metal precursors. The ammonia water (3 wt%) was added dropwise to the solution of metal precursors at 30 °C. The obtained slurry (milk yellow) was aged at 30 °C for 24 h in the solution, keeping the pH around 10, and the hydroxide was filtered, washed, and dried in a convection oven at 110 °C for 24 h. The samples were calcined in air at 700 °C for 5 h.

WO_3/CeZrO and WO_3/ZrO_2 with WO_3 content of 15 wt% were prepared by incipient wetness impregnation method. The aqueous solution of ammonium metatungstate ($[(NH_4)_6(H_2W_{12}O_{40})$–$nH_2O]$, Aldrich Chemical Company) was added to CeZrO and ZrO_2 powder with a solution/powder ratio of 10 mL/g, followed by stirring at room temperature for 12 h, evaporating at 70 °C, and drying at 110 °C for 24 h. The samples were calcined in air at 700 °C for 5 h.

Five supported Pt catalysts with Pt content of 1 wt% (Pt/WO_3/CeO_2/ZrO_2; Pt/ZrO_2, Pt/CeO_2, Pt/CeZrO, Pt/WO_3/ZrO_2, and Pt/WO_3/CeZrO) were also prepared by incipient wetness impregnation method (the same procedure as above WO_3 supporting process), in which tetraammineplatinum ($Pt(NH_3)_4Cl_2$–H_2O, Aldrich Chemical Company) was used as Pt precursor. The samples were calcined in air at 550 °C for 3 h.

2.2. Catalyst characterization

Temperature-programmed experiments were carried out in a conventional flow apparatus (Pulsechemisorb 2705, Micromeritics Inc.), equipped with a thermal conductivity detector (TCD) and a quadruple mass spectrometer (Prisma-QMS200M3). The samples (0.1 g) were degassed in He flow at 200 °C for 2 h, then cooled and stabilized at a temperature. Detailed experimental procedures are described in Table 1.

The BET surface areas were measured by N_2 adsorption using ASAP2010 (Micromeritics Inc.). The samples were degassed at 150 °C, and N_2 adsorption was carried out at 77 K. The crystal structures of prepared samples were confirmed by powder X-ray diffraction (XRD) pattern using monochromic Cu Kα radiation (Rigaku, D/MAX III).

Also Pulsechemisorb 2705 (Micromeritics Inc.) with a thermal conductivity detector was used to determine the Pt dispersions. The amount of CO adsorbed on Pt was determined on Pulsechemisorb 2705 by an ordinary CO pulse method and an O_2–CO_2–H_2–CO pulse method newly proposed by Takeguchi et al. [25]. The details of each procedure are explained in the following:

- Ordinary CO pulse method: The catalyst (0.1 g) was degassed in O_2 flow at 300 °C for 1 h, then cooled down to 30 °C and flushed with He for 10 min. The catalyst was reduced from 30 to 400 °C in H_2(5%)/Ar flow at a heating rate of 10 °C/min, then flushed with He at 400 °C for 10 min. After the sample was cooled down to 30 °C, 0.1 mL of CO was pulsed every 3 min until the intensity of the peak was a constant value.
- O_2–CO_2–H_2–CO pulse method: The catalyst (0.1 g) was degassed in O_2 flow at 300 °C for 1 h, then cooled down to 30 °C and flushed with He for 10 min. Temperature-programmed reduction (TPR) was carried out in H_2(5%)/Ar flow at a heating rate of 10 °C/min and was stopped as soon as the first reduction peak ended. After the sample was cooled down to 30 °C, it was flushed with He for 10 min and was exposed to O_2 flow for 10 min. CO_2 was fed to the sample for 10 min, and then purged with He for 10 min. H_2(5%)/Ar gas was fed to the sample for 10 min, and then purged with He for 1 h. 0.1 mL of CO was pulsed every 3 min until the intensity of the peak was a constant value.

A chemisorption stoichiometry ratio, CO:Pt, of 1:1 was assumed for both cases.

2.3. Catalytic activity measurement

The catalytic activity was measured using a fixed-bed flow reactor at atmospheric pressure. Prior to each reaction, the catalysts (0.5 g) were pretreated in O_2(5%)/He flow at 550 °C for 2 h. A feed gas mixture of CO, NO and O_2 passed through the catalyst bed, and He was used to balance the total flow rate to 260 mL/min (GHSV = 40,000 h^{-1}). Two kinds of reaction modes were employed: (1) NO + CO reaction in the absence of oxygen (feed: CO(0.5%), NO(0.5%)/He); (2) NO + CO reaction in the presence of excess oxygen (feed: CO(0.5%), NO(0.5%), O_2(2%)/He). Catalyst bed temperature was raised at a rate of 2 °C/min from room temperature to 600 °C under continuous flow of reactant stream. The effluent gas was analyzed by on-line gas chromatographs (column: Molecular Sieve 5A & Porapak Q) equipped with TCD for the analysis of CO, O_2, N_2 and N_2O. NO_x analyzer was employed to analyze the concentration of NO and NO_2. NO conversion to N_2 + N_2O was defined as follows:

$$\text{NO conversion to} N_2 + N_2O\,(\%) = 2(y_{N_2,\text{out}} + y_{N_2O,\text{out}})/y_{NO,\text{in}} \times 100$$

where $y_{i,in}$ and $y_{i,out}$ are the mole fraction of compound i at inlet and outlet of reactor, respectively.

3. Results and discussion

3.1. Catalyst characterization

Fig. 1 displayed the XRD patterns of the catalysts. Monoclinic and tetragonal phases of zirconia were identified in the Pt/ZrO_2

Table 1
The detailed procedures of temperature-programmed experiments

Experiments	Procedures
NH_3-TPD	Pretreatment in O_2(5%)/He flow at 550 °C for 1 h, purge in He flow at 30 °C for 1 h, then NH_3 adsorption at 80 °C for 30 min, purge in He flow at 100 °C for 1 h, then NH_3-TPD in He flow (10 °C/min)
H_2-TPR	Pretreatment in O_2(5%)/He flow at 550 °C for 1 h, purge in He flow at 30 °C for 1 h, then H_2-TPR in H_2(5%)/Ar flow (10 °C/min)
H_2-TPR after reduction by CO	Pretreatment in O_2(5%)/He flow at 550 °C for 1 h, purge in He flow at 30 °C for 1 h, then reduction by CO at 100 °C for 1 h, purge in He flow at 30 °C for 1 h, then H_2-TPR in H_2(5%)/Ar flow (10 °C/min)
CO-TPD	Pretreatment in O_2(5%)/He flow at 550 °C for 1 h, purge in He flow at 30 °C for 1 h, then CO adsorption at 30 °C for 1 h, purge in He flow at 30 °C for 1 h, then CO-TPD in He flow (10 °C/min)
NO-TPD after reduction by CO	Pretreatment in O_2(5%)/He flow at 550 °C for 1 h, purge in He flow at 30 °C for 1 h, then reduction by CO at 100 °C for 1 h, purge in He flow at 500 °C 1 h, then NO adsorption in NO(0.1%)/He flow at 30 °C for 1 h, purge in He flow at 30 °C for 1 h, then NO-TPD in He flow (10 °C/min)

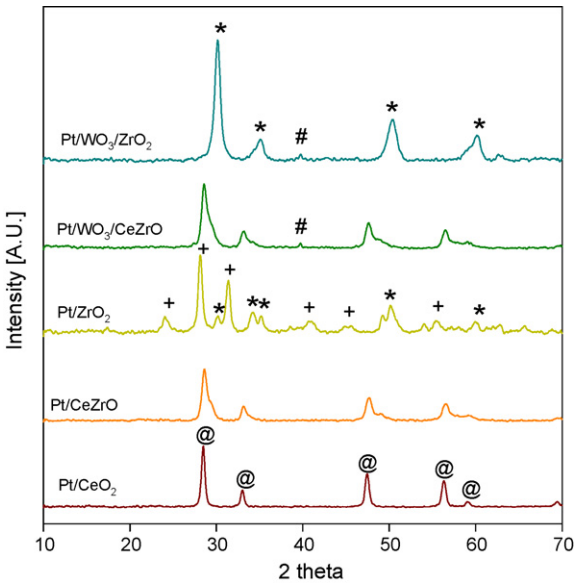

Fig. 1. XRD patterns of various catalysts: (+), monoclinic (ZrO_2); (*), tetragonal (ZrO_2); (@), cubic (CeO_2); (#), monoclinic (WO_3).

sample, whereas only cubic phase of ceria in the Pt/CeO_2. Pt/CeZrO showed a similar phase to Pt/CeO_2, but the characteristic peaks of ceria were progressively shifted to larger angles due to the contraction of lattice cell parameter by insertion of ZrO_2 into CeO_2 fluorite lattice [10–11,26]. The small shoulders on the right side of main peaks were observed and it could evidence the formation of two solid solutions of CeO_2–ZrO_2 such as Ce-rich solid solution for the most part and Zr-rich solid solution in the rest. For Pt/WO_3/CeZrO and $Pt/WO_3/ZrO_2$, the characteristic peak of monoclinic WO_3 phase found at 39° was very weak, indicating that WO_3 was not crystallized to large particles in spite of high loading of 15 wt%. Zirconia stabilizes the tungsten oxide species and WO_3 can be well dispersed on the surface of zirconia [27]. Some studies also showed that WO_3 was well dispersed on zirconia support [28,29]. None of Pt diffraction peaks was observed in the XRD patterns of all catalysts, and this is mainly owing to the low loading of Pt metal (1.0 wt%) or the small particle size below the detection limit of this technique.

BET specific surface areas and Pt dispersion of the catalysts were summarized in Table 2. Pt/CeO_2 had a similar surface area as Pt/ZrO_2, both of which were higher than that of Pt/CeZrO. It was noted that the introduction of WO_3 enhanced their surface area, especially for ZrO_2 support (from 31.2 to 52.2 m^2/g).

The ordinary CO pulse method and the O_2–CO_2–H_2–CO pulse method were used to determine the Pt dispersions. Because CO interacted with not only Pt but also ceria-related supports, the dispersions of Pt on ceria-related supports could be overestimated. Using the O_2–CO_2–H_2–CO pulse method proposed by Takeguchi et al. [25], the interaction between CO and ceria-related support was suppressed and the more exact dispersion of Pt was measured.

Table 2
BET surface area and Pt dispersion of various catalysts: (a) measured by O_2–CO_2–H_2–CO pulse method, (b) measured by ordinary CO pulse method

Catalyst	Surface area (m^2/g)	Pt dispersion[a] (%)	Pt dispersion[b] (%)
Pt/CeO_2	33.3	66.5	–
Pt/ZrO_2	31.2	24.2	25.8
Pt/CeZrO	21.7	57.9	–
$Pt/WO_3/ZrO_2$	52.2	3.0	3.3
Pt/WO_3/CeZrO	28.4	2.0	1.6

In this work, the dispersions of Pt on Pt/CeO_2 and Pt/CeZrO were measured by the O_2–CO_2–H_2–CO pulse method. Ceria was suggested to promote the noble metal dispersion [30,31], and in this work, Pt/CeO_2 and Pt/CeZrO also had relatively high dispersions of Pt. The dispersions of Pt on Pt/ZrO_2, $Pt/WO_3/ZrO_2$, and Pt/WO_3/CeZrO were measured by both the ordinary CO pulse method and the O_2–CO_2–H_2–CO pulse method for comparison in their confidence, and the dispersions measured by both methods were similar with each other. The WO_3-loaded catalysts, $Pt/WO_3/ZrO_2$ and Pt/WO_3/CeZrO, had very low dispersions of Pt.

As reported by Lukinskas et al. [32], Pt dispersions in Pt-impregnated tungstated zirconia catalysts decreased greatly, especially after calcinations at high temperatures above 550 °C. Higher temperatures of calcination (but below 500 °C) most probably increase the rate of surface migration leading to more extensive "embedding" of Pt atoms, and Pt dispersions decreased but still were high. However, the electronic effect cannot be excluded. The calcinations at higher temperatures (above 550 °C) led to sintering of Pt particles. At those temperatures (≥550 °C), the mobility of Pt particles is high enough to escape the surrounding matrix and to agglomerate, and Pt dispersions decreased greatly. In this work, WO_3-loaded samples (WO_3/ZrO_2 and WO_3/CeZrO) after calcination at 700 °C were impregnated with Pt precursor, and the supported Pt catalysts were calcined at 550 °C. It was inferred for this reason that Pt dispersions in the WO_3-loaded catalysts ($Pt/WO_3/ZrO_2$ and Pt/WO_3/CeZrO) were very low.

The NH_3-TPD profiles of the catalysts were displayed in Fig. 2. Compared with Pt/CeO_2 and Pt/CeZrO, Pt/ZrO_2 exhibited more acidity. The introduction of WO_3 into ZrO_2 greatly improved its acid capacity, whereas for CeZrO sample the WO_3 addition just slightly increased the acidic capacity. The super-acidic site was mainly attributed to the double bond character of W=O bond in the complex formed by the interaction of tetragonal phase ZrO_2 with tungstate [33,34]. For Pt/WO_3/CeZrO catalyst, the solid solution formation in CeZrO (see Fig. 1) would significantly inhibit the formation of W=O bond and also restrict the great improvement in its acidity. Also weak acidity was observed in $Pt/WO_3/ZrO_2$ and Pt/WO_3/CeZrO, compared with Pt/ZrO_2 and Pt/CeZrO, respectively.

Fig. 3(a) showed the TPR profiles of the Pt catalysts. The noble metals such as Pt, Pd, and Rh play an important role to improve the reduction property of CeO_2 and CeO_2–ZrO_2 mixed oxide because it can activate the reducing agent, i.e. H_2 [11,35,36]. Three reduction peaks around 160, 250 and 780 °C were observed on Pt/CeO_2

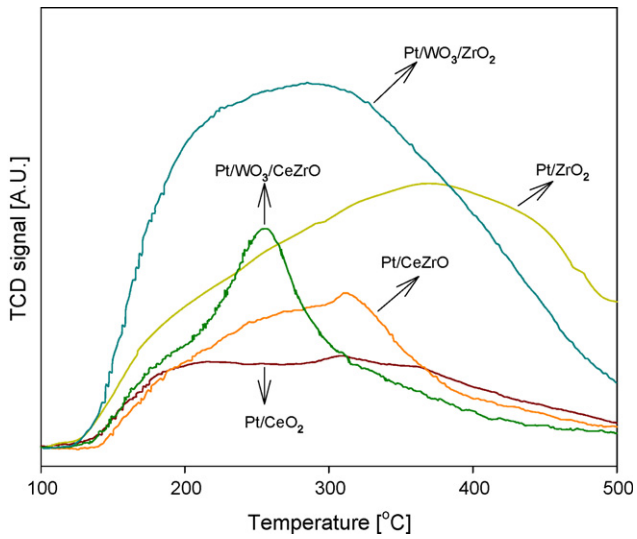

Fig. 2. NH_3-TPD profiles of various catalysts.

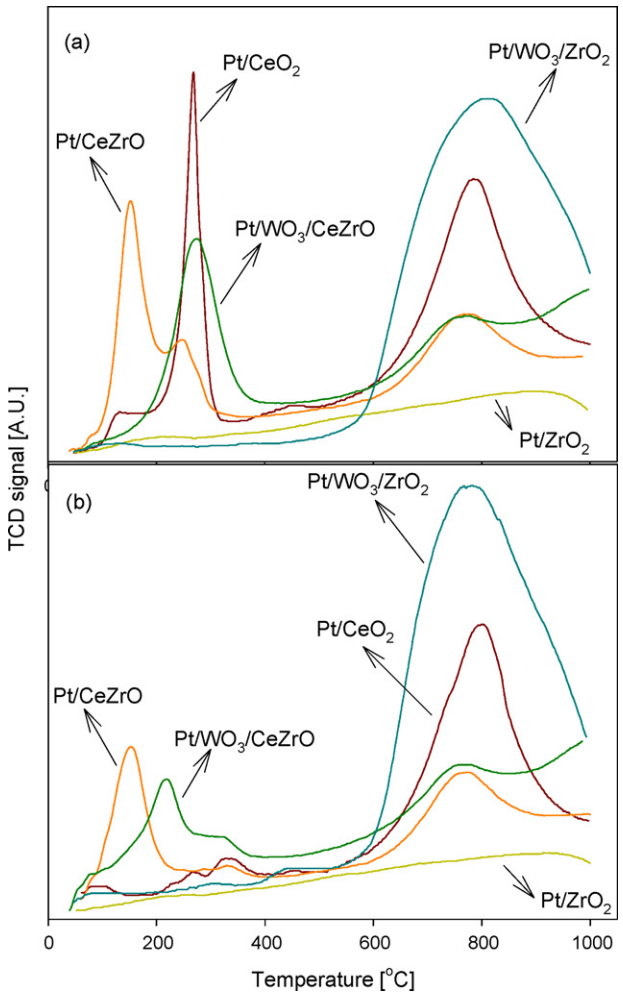

Fig. 3. TPR profiles of various catalysts: (a) without reduction by CO; (b) TPR after reduction by CO at 100 °C for 1 h.

sample, which correspond to the reduction of surface Pt, surface Ce and bulk Ce, respectively [35]. It seemed appropriate that the small reduction peak around 160 °C was attributed to surface Pt with little loading. The similar TPR profile was observed on Pt/CeZrO sample. Compared with Pt/CeO_2, Pt/CeZrO exhibited a higher intensity of Pt reduction peak but a lower intensity of surface Ce reduction peak. Some studies [11,12] suggested the fundamental relationships between redox properties and structures in CeO_2–ZrO_2 mixed oxides; insertion of progressively increasing amount of ZrO_2 into the CeO_2 fluorite lattice was responsible for a progressive increase of structural defects for the oxygen migration in the lattice, so that the Zr addition into CeO_2 lattice enhanced the Ce reduction [11,37]. Noticeably, the hydrogen uptake of Pt/CeZrO for the reduction peak at 160 °C was much larger than that expected for the reduction of all platinum, and the peak could be due to the concomitant reduction of little PtO_x crystallites and surface Ce with enhanced reducibility by the Zr addition. No obvious Pt reduction peak was observed on $Pt/WO_3/CeZrO$, $Pt/WO_3/ZrO_2$, and Pt/ZrO_2 samples. WO_3 reduction took place at a high temperature similar to that of bulk Ce.

TPR profiles of the catalysts after pre-reduction by CO at 100 °C were illustrated in Fig. 3(b). For Pt/CeO_2 and Pt/CeZrO catalysts, the reduction peaks of 250 °C decreased sharply, whereas other reduction peaks changed very little. It was deduced that the surface Ce active sites would be the preferable sites for CO adsorption and reduced by CO more easily. In contrast with Pt/

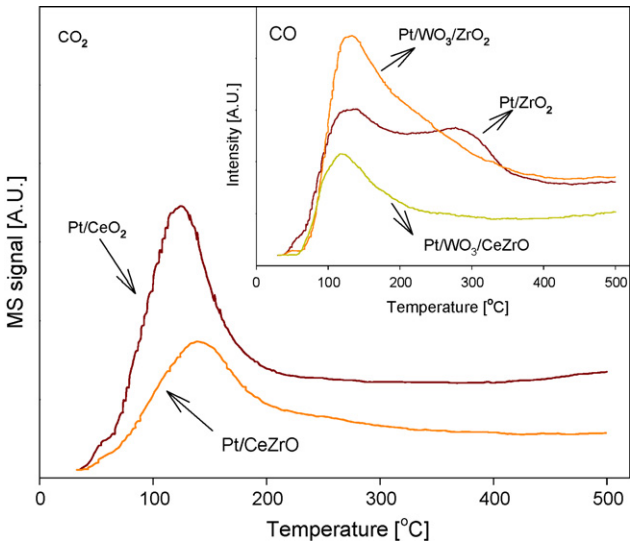

Fig. 4. CO-TPD profiles of various catalysts.

CeO_2 and Pt/CeZrO, $Pt/WO_3/CeZrO$ still showed a high reduction peak of 160 °C even after pre-reduction by CO, which showed that WO_3 introduction into CeZrO inhibited the surface reduction of the catalyst.

Fig. 4 represented the CO-TPD profiles over the five Pt supported catalysts. Since the catalysts used in this work were all in their oxidized states, their oxidized surface tended to oxidize

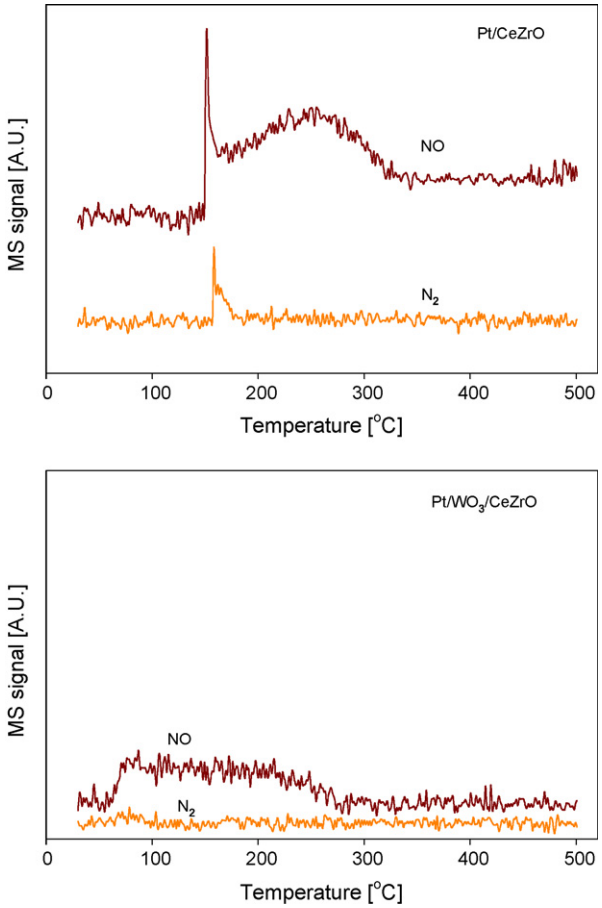

Fig. 5. NO-TPD profiles of Pt/CeZrO and $Pt/WO_3/CeZrO$ catalysts after reduction by CO at 100 °C for 1 h.

the adsorbed CO to CO_2. Only CO_2 desorption was observed over Pt/CeO_2 and Pt/CeZrO, while just CO was desorbed from other three samples. This reveals that CO can be oxidized on the surface of Pt/CeO_2 and Pt/CeZrO more easily. This result was coincident with TPR results of Fig. 3, where Pt/CeO_2 and Pt/CeZrO were reduced by CO more easily.

NO-TPD profiles of Pt/CeZrO and Pt/WO_3/CeZrO catalysts after reduction by CO at 100 °C were illustrated in Fig. 5. NO was reduced to N_2 easily over Pt/CeZrO catalyst, while N_2 product was almost negligible over Pt/WO_3/CeZrO catalyst. According to TPR and CO-TPD, it was inferred that Pt/WO_3/CeZrO catalyst was hardly reduced completely after pre-reduction by CO and had to remain in the oxidized state. Before NO-TPD was carried out, the catalysts were pre-reduced by CO at 100 °C like TPR. The reduction of NO to N_2 hardly took place on the catalyst to remain in the oxidized state even after pre-reduction by CO. NO-TPD profile of Pt/CeO_2 was similar to that of Pt/CeZrO, while only NO desorption was observed over Pt/WO_3/ZrO_2 and Pt/ZrO_2.

3.2. Catalytic activity

Two kinds of reaction modes (NO + CO reaction without or with oxygen) were employed. In order to effectively compare the different catalytic performances, especially when excess oxygen existed, the catalysts employed here were all in oxidized state and not pre-reduced by CO or H_2.

Firstly, NO reduction by CO without oxygen was carried out and the variations in CO and NO conversion with reaction temperature over various catalysts were shown in Fig. 6. Compared with other catalysts (Pt/ZrO_2, Pt/WO_3/ZrO_2, Pt/WO_3/CeZrO), Pt/CeZrO and Pt/CeO_2 exhibited the better catalytic activities. The surface Ce sites on Pt/CeO_2 and Pt/CeZrO were reduced by CO more easily and the reduction of NO could take place on the reduced sites as evidenced from TPR, CO-TPD, and NO-TPD. Accordingly, Pt/CeZrO and Pt/CeO_2 exhibited the better catalytic activities for NO + CO reaction without oxygen. Pt/CeZrO showed higher activity than Pt/CeO_2 in spite of lower Pt dispersion.

It was also evidenced from TPR, CO-TPD, and NO-TPD that WO_3 addition tended to inhibit the surface reduction by CO and the formation of the active sites for NO reduction in the Pt/WO_3/CeZrO catalysts. WO_3 introduction into the easily reducible catalysts such as Pt/CeZrO led to the decrease in their catalytic activity. Pt/WO_3/ZrO_2 showed a slight increase in activity through WO_3 addition even if Pt/ZrO_2 showed the poorest activity for NO + CO reaction without oxygen. As reported by Regalbuto and Wolf [15], Pt-WO_3 adlineation sites had very high NO dissociation activity and increased the activity toward the NO + CO reaction. However, according to the results shown in Figs. 2 and 6, there was no obvious correlation

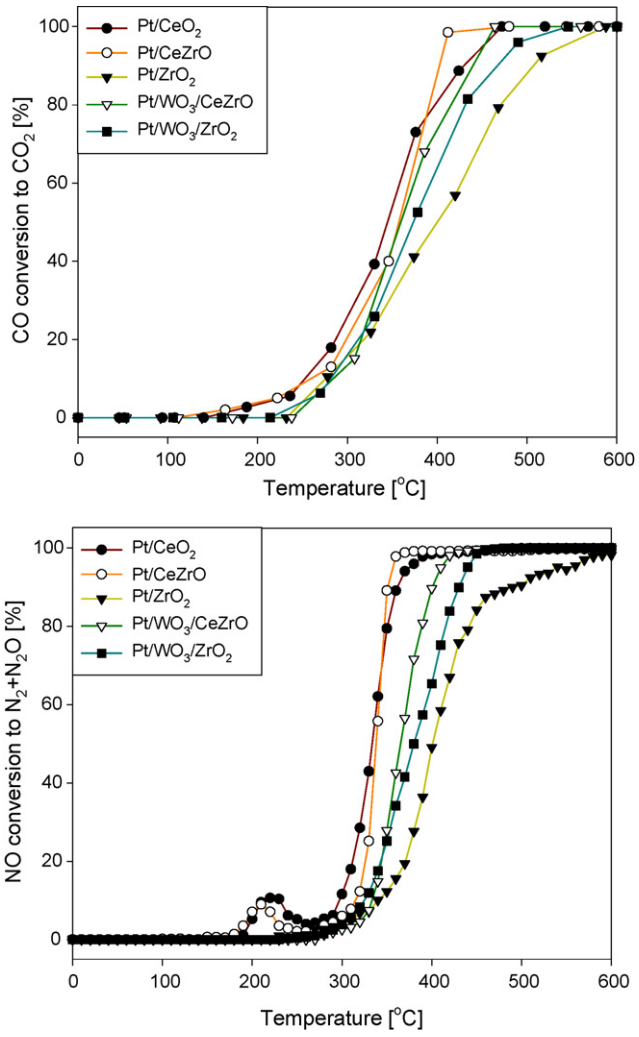

Fig. 6. Catalytic activities for the reduction of NO by CO over various catalysts (CO: 0.5%, NO: 0.5%).

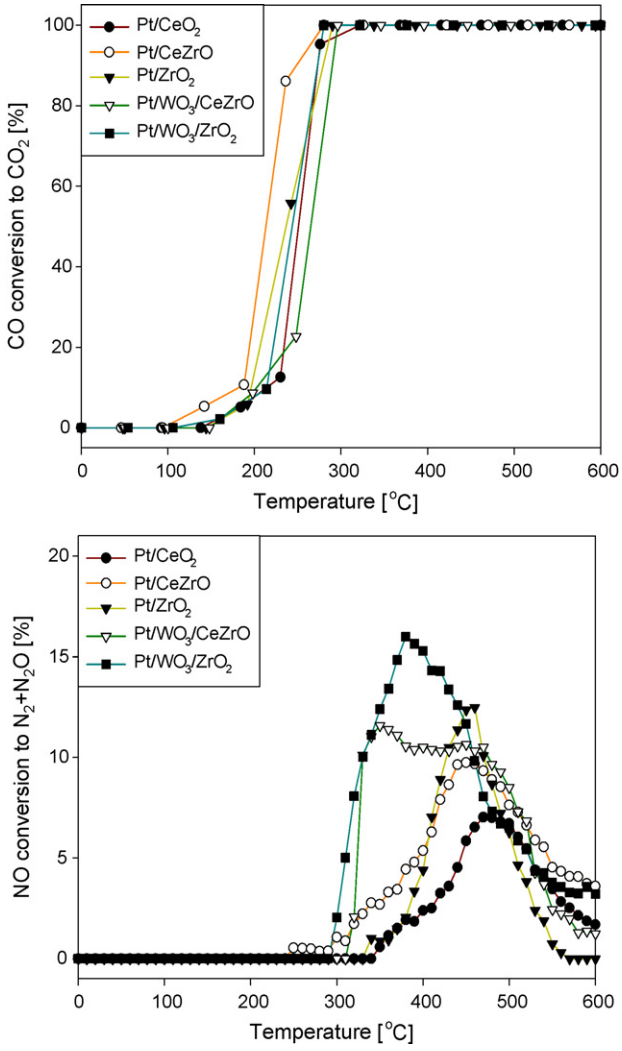

Fig. 7. Catalytic activities for the reduction of NO by CO over various catalysts in the presence of excess oxygen (CO: 0.5%, NO: 0.5%, O_2: 2%).

between acidity and catalytic activity for NO + CO reaction without oxygen over $Pt/WO_3/CeO_2/ZrO_2$ catalysts.

The catalytic reduction of NO by CO with excess oxygen was displayed as light-off curves in Fig. 7. With excess oxygen, CO reacted with O_2 more easily than with NO and the NO conversion was greatly inhibited. NO conversion was less than 18% at maximum over those catalysts, while complete conversion of CO to CO_2 took place below 300 °C. The $Pt/WO_3/CeZrO$ and $Pt/WO_3/ZrO_2$ catalysts exhibited much higher NO conversions especially in the low temperature range of 300–400 °C even if their Pt dispersions were quite low.

However, there seemed to be some correlations between acidity and catalytic activity for NO + CO reaction with excess oxygen over $Pt/WO_3/CeO_2/ZrO_2$ catalysts; the more acidity led to the higher NO conversion, especially in the low temperature range. The acidity from ZrO_2 and WO_3 in $Pt/WO_3/CeO_2/ZrO_2$ catalysts should play an important role on their NO conversion in the presence of excess oxygen.

4. Conclusion

Various supported Pt catalysts ($Pt/WO_3/CeO_2/ZrO_2$; Pt/ZrO_2, Pt/CeO_2, Pt/CeZrO, $Pt/WO_3/ZrO_2$, and Pt/WO_3/CeZrO) were prepared and characterized, and their characteristics of catalytic reductions of NO by CO with or without oxygen were investigated. TPR and CO-TPD showed that Pt/CeO_2 and Pt/CeZrO could be easily reduced by CO while the reduction by CO was inhibited with the introduction of WO_3 in the case of Pt/WO_3/CeZrO. According to NO-TPD, NO reduction could not proceed over the catalysts (Pt/WO_3/CeZrO, Pt/ZrO_2, $Pt/WO_3/ZrO_2$) to remain in an oxidized state even after reduction by CO, but NO reduction was possible over Pt/CeO_2 and Pt/CeZrO catalysts when reduced by CO. For NO + CO reaction without oxygen, those easily reducible catalysts (Pt/CeO_2 and Pt/CeZrO) exhibited better catalytic performances. With excess oxygen, however, Pt/WO_3/CeZrO and $Pt/WO_3/ZrO_2$ catalysts exhibited higher NO conversions to N_2 and N_2O especially at a low temperature. The acidity from ZrO_2 and WO_3 in $Pt/WO_3/CeO_2/ZrO_2$ catalysts should play an important role on their NO conversion only in the presence of excess oxygen.

Acknowledgement

This research was supported financially by the Brain Korea 21 (BK21) program from Korean Ministry of Education.

References

[1] P. Granger, F. Dhainaut, S. Pietrzik, P. Malfoy, A.S. Mamede, L. Leclercq, G. Leclercq, Top. Catal. 39 (2006) 65–76.
[2] T. Kolli, U. Lassi, K. Rahkamaa-Tolonen, T.J.J. Kinnunen, R.L. Keiski, Appl. Catal. A: Gen. 298 (2006) 65–72.
[3] K. Thirunavukkarasu, K. Thirumoorthy, J. Libuda, C.S. Gopinath, J. Phys. Chem. B 109 (2005) 13272–13282.
[4] T. Kolli, K. Rahkamaa-Tolonen, U. Lassi, A. Savimaki, R.L. Keiski, Catal. Today 100 (2005) 297–302.
[5] A.D. Sarkar, B. Khanra, J. Mol. Catal. A: Chem. 229 (2005) 25–29.
[6] P. Granger, C. Dujardin, J.F. Paul, G. Leclercq, J. Mol. Catal. A: Chem. 228 (2005) 241–253.
[7] A.B. Hungria, M. Fernandez-Garcia, J.A. Anderson, A. Martinez-Arias, J. Catal. 235 (2005) 262–271.
[8] G.S. Zafiris, R.J. Gorte, Surf. Sci. 276 (1992) 86.
[9] D. Terribile, A. Trovarelli, J. Llorca, J. Catal. 178 (1998) 229.
[10] J.R. Kim, W.J. Myeong, S.K. Ihm, Appl. Catal. B: Environ. 71 (2006) 57.
[11] P. Fornasiero, R.D. Monte, R. Ranga, J. Kaspar, S. Meriani, A. Trovarelli, M. Graziani, J. Catal. 151 (1995) 168.
[12] G. Vlaic, P. Fornasiero, S. Geremia, J. Kaspar, M. Graziani, J. Catal. 168 (1997) 386.
[13] A. Trovarelli, C. de Leitenburg, G. Dolcetti, Chemtech. 27 (1997) 32.
[14] H. Vidal, J. Kaspar, M. Pijolat, Appl. Catal. B: Environ. 27 (2000) 49.
[15] J.R. Regalbuto, E.E. Wolf, J. Catal. 109 (1988) 12.
[16] R. Perez-Hernandez, F. Aguilar, A. Gomez-Cortes, G. Diaz, Catal. Today 107–108 (2005) 175.
[17] R. Mariscal, S. Rojas, A. Gomez-Cortes, G. Diaz, R. Perez, J.L.G. Fierro, Catal. Today 75 (2002) 385.
[18] A. Boix, R. Mariscal, J.L.G. Fierro, Catal. Lett. 68 (2000) 169.
[19] K.I. Hadjiivanov, Catal. Rev. Sci. Eng. 42 (2000) 71.
[20] Y.H. Chin, W.E. Alvarez, D.E. Resasco, Catal. Today 62 (2000) 159.
[21] Y.H. Chin, W.E. Alvarez, D.E. Resasco, Catal. Today 62 (2000) 291.
[22] A. Ali, Y.H. Chin, D.E. Resasco, Catal. Lett. 56 (1998) 111.
[23] J.O. Petunchi, W.K. Hall, Appl. Catal. B 2 (1993) L17.
[24] C.J. Loughran, D.E. Resasco, Appl. Catal. B 7 (1995) 113.
[25] T. Takeguchi, S. Manabe, R. Kikuchi, K. Eguchi, T. Kanazawa, S. Matsumoto, W. Ueda, Appl. Catal. A 293 (2005) 91.
[26] S.T. Aruna, K.C. Patil, Nanostruct. Mater. 10 (1998) 955.
[27] J.R. Sohn, M.Y. Park, Langmuir 14 (1998) 6140.
[28] W. Sun, Z. Zhao, C. Guo, X. Ye, Y. Wu, Ind. Eng. Chem. Res. 39 (2000) 3717.
[29] D.G. Barton, M. Shtein, R.D. Wilson, S.L. Soled, E. Iglesia, J. Phys. Chem. B 103 (1999) 630.
[30] R.D. Monte, J. Kaspar, Top. Catal. 28 (2004) 47.
[31] J. Kaspar, P. Fornasiero, M. Graziani, Catal. Today 50 (1999) 285.
[32] P. Lukinskas, S. Kuba, B. Spliethoff, R.K. Grasselli, B. Tesche, H. Knozinger, Top. Catal. 23 (2003) 163.
[33] B.Y. Zhao, X.P. Xu, J.M. Gao, H.R. Ma, Y.Q. Tang, Acta Phys. Chim. Sin 11 (1995) 979.
[34] J.R. Sohn, J.S. Han, J. Ind. Eng. Chem. 3 (2005) 439.
[35] C. de Leitenburg, A. Trovarelli, J. Kaspar, J. Catal. 166 (1997) 98.
[36] R.D. Monte, P. Fornasiero, M. Graziani, J. Kaspar, J. Alloys Comp. 275–277 (1998) 877.
[37] F. Fally, V. Perrichon, H. Vidal, J. Kaspar, G. Blanco, J.M. Pintado, S. Bernal, G. Colon, M. Daturi, J.C. Lavalley, Catal. Today 59 (2000) 373.